Spectral Network Principle for Frequency Synchronization in Repulsive Laser Networks

Mostafa Honari-Latifpour,[1,2] Jiajie Ding,[1,2] Igor Belykh,[3] and Mohammad-Ali Miri[1,2,*]

[1]*Department of Physics, Queens College, City University of New York, New York, New York 11367, USA*
[2]*Physics Program, The Graduate Center, City University of New York, New York, New York 10016, USA*
[3]*Department of Mathematics & Statistics and Neuroscience Institute,*
Georgia State University, P.O. Box 4110, Atlanta, Georgia, 30302-410, USA

(Dated: October 7, 2024)

Network synchronization of lasers is critical for achieving high-power outputs and enabling effective optical computing. However, the role of network topology in frequency synchronization of optical oscillators and lasers remains not well understood. Here, we report our significant progress toward solving this critical problem for networks of heterogeneous laser model oscillators with repulsive coupling. We discover a general approximate principle for predicting the onset of frequency synchronization from the spectral knowledge of a complex matrix representing a combination of the signless Laplacian induced by repulsive coupling and a matrix associated with intrinsic frequency detuning. We show that the gap between the two smallest eigenvalues of the complex matrix generally controls the coupling threshold for frequency synchronization. In stark contrast with attractive networks, we demonstrate that local rings and all-to-all networks prevent frequency synchronization, whereas full bipartite networks have optimal synchronization properties. Beyond laser models, we show that, with a few exceptions, the spectral principle can be applied to repulsive Kuramoto networks. Our results provide guidelines for optimal designs of scalable optical oscillator networks capable of achieving reliable frequency synchronization.

I. INTRODUCTION

Frequency synchronization when coupled photonic oscillators with different natural frequencies synchronize to a common frequency is a critical requirement for unconventional computing using optical oscillators and lasers [1–5] as well as for communication, sensing, and metrology [6]. Frequency synchronization implies phase entrainment with non-stationary yet bounded relative phases. Such average frequency locking without phase locking accompanies resonance-assisted synchronization in coupled lasers [7]. While phase synchronization is crucial for coherent beam combining in high-power laser systems [8, 9], frequency synchronization is essential in applications where optical oscillators with initially different emission frequencies need to operate coherently. In particular, in optical computing architectures and photonic neural networks, arrays of lasers with intrinsic frequency detuning perform complex computations through interference and modulation [10]. Frequency synchronization ensures that the computational elements interact coherently, maintaining the integrity of the computational processes. In optomechanical systems, optical oscillators with different frequencies interact with mechanical resonators [11], where frequency synchronization enhances the system's sensitivity and performance. Similarly, in optical frequency combs used for precision measurements and metrology, frequency synchronization across the comb lines is vital [12, 13]. Trapped Bose-Einstein condensates that simulate the classical spin degrees of freedom in the XY Hamiltonian require frequency synchronization for properly operating the XY simulator [14].

Complex laser oscillator networks that expand beyond the conventional lattice geometries based on the evanescent tail coupling of the neighboring lasers can be implemented using diffraction engineering [15–17]. The main types of coupling in laser networks encompass dispersive and dissipative interactions. Dissipative coupling induces the splitting of the resonant frequencies and is generally considered the superior mechanism for promoting network synchronization [18]. However, the dissipative coupling can be attractive or repulsive, promoting in-phase and out-of-phase oscillations, respectively. The significance of the repulsive coupling scenario manifests itself in various applications, including the spin models for unconventional computing [1, 19, 20]. In this context, the attractive coupling corresponds to the trivial ferromagnetic case. In contrast, repulsive coupling aligns with anti-ferromagnetism that can embed hard optimization problems [3, 14, 21], and can represent non-trivial energy-based neural network models [22]. Furthermore, it has been suggested that anti-phase-coupled lasers can have better overall beam combining efficiencies [23].

Extensive research has been devoted to the role of network structure and parameter heterogeneity on the synchronization in oscillator networks with attractive coupling, including laser arrays [9, 24–29], and more broadly, Laplacian [30–37], pulse-coupled [38–42], amplitude-phase oscillator [43–46] and Kuramoto-type networks [34, 47–56]. In particular, it was shown that the critical coupling for the onset of phase synchronization in Kuramoto oscillator networks of nonidentical oscillators is controlled by the largest eigenvalue of the adjacency matrix [34]. Complete synchronization in Laplacian networks of identical [30] or nonidentical [33, 37, 57] oscillators is determined via the master stability function that involves the second largest and the largest eigenvalues of

the Laplacian matrix [30].

However, a significant knowledge gap remains regarding the interplay of these factors for phase-locked rhythms or frequency synchronization in repulsive oscillator networks. Such networks exhibit different forms of phase and frequency synchronization, including splay states [58], clusters [59], and cyclops states [60] whose dependence on the network structure is not well understood and can be counterintuitive. For example, globally coupled repulsive Kuramoto networks fail to reach frequency synchronization, whereas it occurs in locally coupled networks [61]. Generally, the governing principles for the transition to phase-locked patterns and frequency synchronization in repulsive networks cannot be inferred from their counterparts with attractive coupling.

This paper primarily focuses on frequency synchronization in optical oscillator networks with intrinsic frequency detuning, which is a foundational step before achieving phase-locking regimes in many oscillatory systems [62]. This paper extends our previous study of frequency synchronization of two class-A laser oscillators with dissipative coupling [18] to larger networks. We reveal a general principle that pairs frequency synchronization with the network structure and parameter detuning in networks of class-A laser oscillators [63, 64] with repulsive signless Laplacian dissipative coupling [18]. This principle indicates that the coupling threshold for frequency synchronization is controlled by the spectral knowledge of the complex matrix composed of the connectivity matrix and the matrix representing intrinsic frequency detuning. More precisely, the coupling threshold in such repulsive laser networks is defined by the spectral gap between the two smallest (non-zero) eigenvalues of the complex matrix. This principle suggests that full bipartite networks rather than global or local network topologies provide optimal synchronization properties. In particular, we demonstrate that dense long-range interactions do not necessarily lower the synchronization threshold. We also show that the dynamics of the amplitude-phase laser oscillators with signless Laplacian dissipative coupling can be approximated by the Kuramoto model with repulsive coupling. As a result, with a few notable exceptions, the spectral network principle can also be applied to frequency synchronization in such Kuramoto networks. Our results may open the door to optimal designs of scalable optical computing networks that require their photonic oscillators to be frequency synchronized to be used as analog processors [3, 4].

The layout of this paper is as follows. Section II introduces the laser network model and states the problem under consideration. In Sec. III, we formulate the spectral network principle for networks of identical laser oscillators. In Sec. IV, we extend our results to non-identical oscillators. In Sec. V, we demonstrate how the principle applies to frequency synchronization in repulsive Kuramoto networks. Sec. VI contains concluding remarks and discussions.

II. THE MODEL

We consider a network of N dissipatively coupled lasers described by a minimal dynamical model that involves only the amplitude and phase of the field in each laser cavity [65]. The complex amplitude of the nth oscillator obeys

$$\dot{a}_n(t) = (-i\omega_n - 1 + g_0(1 - |a_n|^2))a_n, \ n = 1, ..., N, \quad (1)$$

where time is normalized to the field decay rate, ω_n and g_0 represent the dimensionless resonant frequency and small signal gain, respectively. This model applies to class-A lasers, where the atomic degrees of freedom can be adiabatically eliminated due to their much faster decay rates compared to that of the electromagnetic field [63, 64]. In this regime, the laser dynamics's description simplifies to a single equation governing the evolution of the electric field with an appropriate saturable gain term [66]. Although semiconductor lasers are typically classified as class-B lasers — requiring models that account for the complex dynamic interplay between the field and population inversion [67] — it is noteworthy that near the oscillation threshold, a class-B laser's behavior can be approximated using a class-A laser model [68]. Moreover, the simplicity and analytical tractability of the class-A laser model make it valuable in various applications—including optical neural computing [69], quantum simulations [70], and topological lasers [71] — which supports its use in exploring synchronization phenomena in optical networks. From a nonlinear dynamics perspective, the behavior of the model (1) is analogous to that of the Landau-Stuart oscillator.

The dynamical equations governing complex field amplitudes of the network are

$$\dot{\mathbf{a}}(t) = -\mathbf{a} + g_0(1 - \mathbf{a}^* \cdot \mathbf{a})\mathbf{a} - i\Omega\mathbf{a} - \kappa Q\mathbf{a}, \quad (2)$$

where $\mathbf{a} = [a_1, ..., a_N]^T$ is the vector containing the lasers complex amplitudes, $\Omega = \text{diag}(\omega_1, ..., \omega_N)$ is an $N \times N$ diagonal matrix involving detuned resonant frequencies, Q is the signless Laplacian connectivity matrix with off-diagonal elements $q_{mn} = 1$ for coupled oscillators and $q_{mn} = 0$ otherwise, and diagonal elements $q_{mm} = \sum_{m \neq n} q_{mn}$. Figure 1 illustrates the physical implementation of the laser oscillator network (2). Figure 1(a) schematically depicts the interaction of two laser oscillators through the dissipative coupling. In this setting, the energy exchange between two laser cavities is mediated through the surrounding medium, where radiation leakage is inevitable. The in-phase emission of the two oscillators in the decay channel yields the negative sign of the coupling term $-\kappa Q\mathbf{a}$ in (2) with the coupling coefficient $\kappa > 0$. As a result, it makes the dissipative coupling repulsive (see [18] for a more detailed description of the dissipative coupling's role in frequency synchronization of two class-A laser oscillators). Larger networks with arbitrary connections defined by the signless Laplacian matrix Q can be implemented by diffraction engineering [15] as depicted in Fig. 1(b),(c).
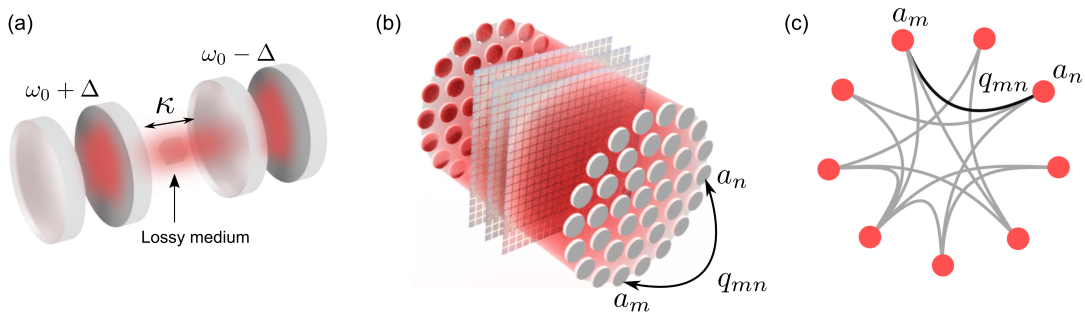
FIG. 1. (a) The concept of dissipative coupling, where two resonators with mismatched resonant frequencies ($\omega_0 + \Delta$ and $\omega_0 - \Delta$) interact through a dissipative (lossy) medium, which causes radiation leakage. (b) The general scheme for creating arbitrary coupling between spatially-segmented laser oscillators (gray dots) through intra-cavity diffraction engineering. The diffractive surfaces (three transparent meshes) steer light from individual lasers toward other lasers to implement, through transverse coupling (red dots), an arbitrarily complex network topology within the array. (c) The equivalent connection graph of system (2).
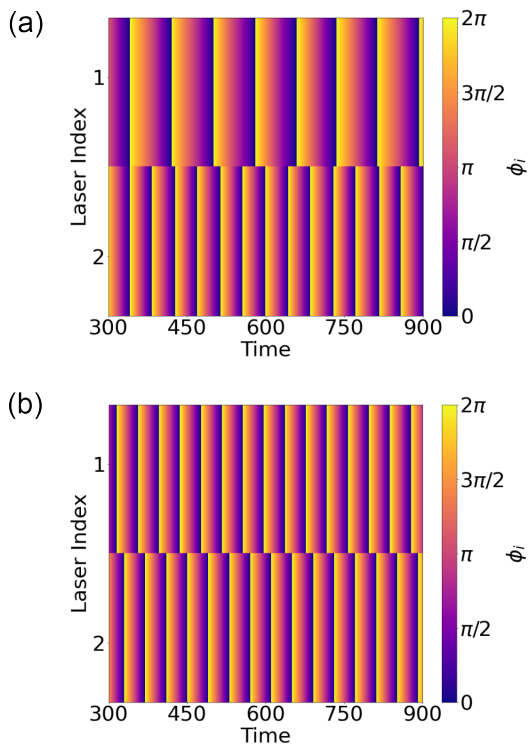

FIG. 2. The onset of frequency synchronization in the two-oscillator network (4). The color plots indicate the oscillators' phases. (a). Below the synchronization coupling threshold, $\kappa = 0.01 < \kappa_c$. (b). Frequency synchronization above the coupling threshold $\kappa = 0.06 > \kappa_c$. Parameters $\omega_1 = \omega_0 + \Delta$, $\omega_1 = \omega_0 - \Delta$, where $\omega_0 = 1$, $\Delta = 0.05$, and $g_0 = 1.02$.

Combining the last two terms in (2), we introduce the complex matrix

$$M = i\Omega + \kappa Q, \qquad (3)$$

which accounts for the contribution of intrinsic frequency detuning and linear dissipative coupling. In an amplitude and phase representation of the complex amplitudes $a_n(t) = A_n(t)e^{i\phi_n(t)}$, the network (2) can be written in the form

$$\dot{A}_n = -A_n + g_0(1 - A_n^2)A_n - \kappa \sum_{m=1}^{N} q_{mn} A_m \cos(\phi_m - \phi_n),$$

$$\dot{\phi}_n = -\omega_n - \kappa \sum_{m=1}^{N} q_{mn} \frac{A_m}{A_n} \sin(\phi_m - \phi_n), \ n = 1, ..., N.$$

$$(4)$$

Under the simplifying assumption that the amplitudes of all laser oscillators settle down to the same value so that $A_n(t) \to 1$, the system (4) can be reduced to the classical repulsive Kuramoto model with an arbitrary adjacency matrix $C = Q - q_{mm}I$, where $q_{mm}I$ is the degree matrix of the connection graph. However, as we will demonstrate in Sec. V, the dynamics of the Kuramoto model and the full system can be quite different.

Frequency synchronization occurs in the network (4) when $\langle \dot{\phi}_1 \rangle = \langle \dot{\phi}_2 \rangle = ... = \langle \dot{\phi}_N \rangle$, where $\langle ... \rangle$ denotes a time average. Hereafter, we will be using an order parameter $R = \frac{2}{N(N-1)} \langle \sum_{i<j}^{N} \exp\{-(\dot{\phi}_i - \dot{\phi}_j)^2\} \rangle$ as a measure for the degree of frequency coherence. According to our definition, $R = 1$ corresponds to perfect frequency synchronization that may include phase-locked patterns with possibly stationary relative phases. Such examples include splay states [58] and cyclops states [60]. Typically, frequency synchronization emerges when the coupling exceeds a critical threshold value κ_c. For the two-oscillator network (2) with frequency detunings $\omega_1 = \omega_0 - \Delta$ and $\omega_2 = \omega_0 + \Delta$, the threshold coupling can be calculated analytically so that $\kappa_c = \Delta$ [18]. Figure 2 demonstrates the dynamics below and above the coupling threshold.

In the following, we demonstrate that not all network topologies support frequency synchronization, even for identical oscillators and infinitely strong coupling. To do so, we first derive the spectral network principle for networks of identical laser oscillators and connect the coupling threshold κ_c with the spectrum of the signless

Laplacian matrix Q.

III. IDENTICAL LASER OSCILLATORS

Previous studies used energy Lyapunov-type functions to derive conditions on the stability of frequency synchronization in the classical Kuramoto model with non-identical oscillators and global attractive coupling [50] or local repulsive coupling [61]. However, constructing such functions for the amplitude-phase model (2) with arbitrary repulsive coupling is elusive. Here, we use an alternative approach to making sense of the complex matrix M's spectral properties as a network synchronizability criterion. We view the onset of frequency synchronization as competition between the network eigenmodes for oscillation. This can be better understood in the case of identical oscillators, i.e., when $\omega_1 = \omega_2 = \cdots = \omega_N = \omega_0$. In this case, considering the dynamics starting at low field intensities $|\mathbf{a}| \ll \mathbf{1}$, the evolution can be linearized in the rotating frame of ω_0 as

$$\dot{\mathbf{a}} = (g_0 - 1)\mathbf{a} - \kappa Q \mathbf{a}. \tag{5}$$

The connectivity matrix Q has N real eigenvalues $s_1 \leq s_2 \leq ... \leq s_N$. Diagonalizing (5) using the eigenmode basis of Q, $\mathbf{a}(t) = \sum_m \alpha_m(t)\mathbf{v}_m$, where $\alpha_m(t) = \mathbf{v}_m^\dagger \mathbf{a}(t)$, we obtain the evolution equation for the mth eigenmode

$$\dot{\alpha}_m(t) = (g_0 - \kappa s_m - 1)\alpha_m, \; m = 1, ..., N. \tag{6}$$

The fundamental mode ($m = 1$) with the maximum net small-intensity gain, $g_0 - \kappa s_1 - 1$, has a higher probability of becoming the lasing mode, thereby inducing frequency synchronization. To do so, it needs to win the lasing competition with its closest competing mode with $m = 2$ and the gain $g_0 - \kappa s_2 - 1$. The outcome of this competition is generally controlled by the gain difference between the two modes, $\kappa(s_2 - s_1)$, that has to exceed an energy threshold. This suggests that the threshold coupling, κ_c, for the onset of frequency synchronization can be estimated as

$$\kappa_c = \frac{b}{s_2 - s_1} \equiv \frac{b}{\gamma}, \tag{7}$$

where s_1 and s_2 are the first and second smallest eigenvalues of the signless Laplacian matrix Q, and b is a scaling factor. Note that the spectral network principle (7) for frequency synchronization in repulsive networks (2) is in sharp contrast with the existing spectral network conditions for phase synchronization in Kuramoto networks controlled by the adjacency matrix's largest eigenvalue [34] and complete synchronization in Laplacian networks [30] determined by the connectivity matrix's second largest and largest eigenvalues. In particular, the spectral gap $\gamma = s_2 - s_1$ is zero for the globally coupled network (2), so frequency synchronization cannot be achieved even for large values of κ. On the contrary, global Kuramoto or Laplacian networks with
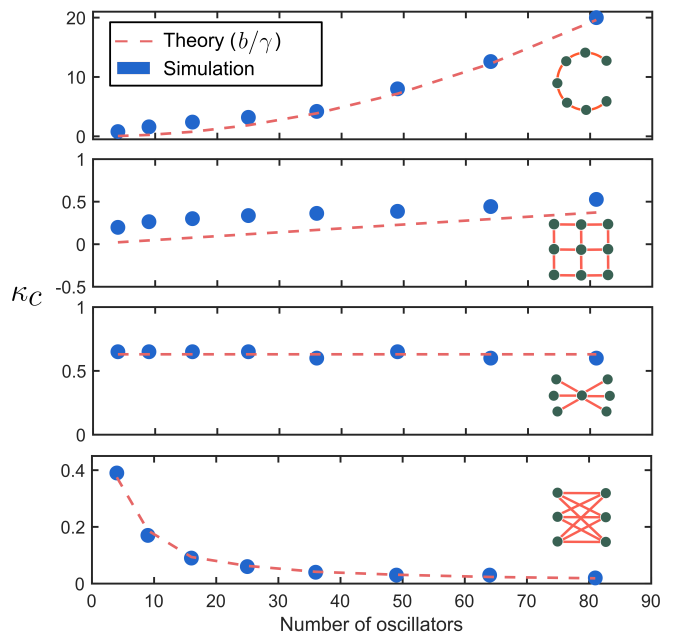

FIG. 3. Actual (blue circles) and predicted (red dashed line) frequency synchronization threshold κ_c (with the order parameter $R > 0.99$) in common bipartite network topologies, ranging from sparse to dense graphs. The predicted thresholds are computed from the spectral principle (7) with the scaling parameter b chosen to fit the data. Parameters are $\omega_0 = 1$ and $g_0 = 6.5$. The fitting parameter b is set to 0.0295, 0.045, 0.63, and 0.75 for the chain, square, star, and full bipartite topologies, respectively.

attractive coupling are known to have the best synchronization properties, determined by the lowest coupling threshold for phase and complete synchronization. At the same time, the spectral network principle (7) agrees with the observation that repulsive Kuramoto networks of identical oscillators can not be frequency-synchronized [61].

Similarly, networks with the zero spectral gap, $\gamma = 0$, are expected to be non-synchronizable. The property that guarantees a non-zero spectral gap is the bipartiteness of the graph associated with the matrix Q. It has been previously shown in the context of spectral signless Laplacian graph theory [72–74] that the more edges need to be removed to make the graph bipartite, the larger the smallest eigenvalue [75] and the smaller the spectral gap are. Therefore, a bipartite graph that generally is the easiest to synchronize has its smallest eigenvalue at zero, leading to a larger spectral gap. To support this claim and validate the predictive power of the spectral network principle (7), we numerically studied the scaling of the synchronization threshold κ_c as a function of the network size in four common network topologies, ranging from sparse to dense graphs (Fig. 3). All four types of networks discussed here are bipartite graphs and, hence, synchronizable. For all these networks, the spectral gap γ can be calculated analytically as a function of N. For
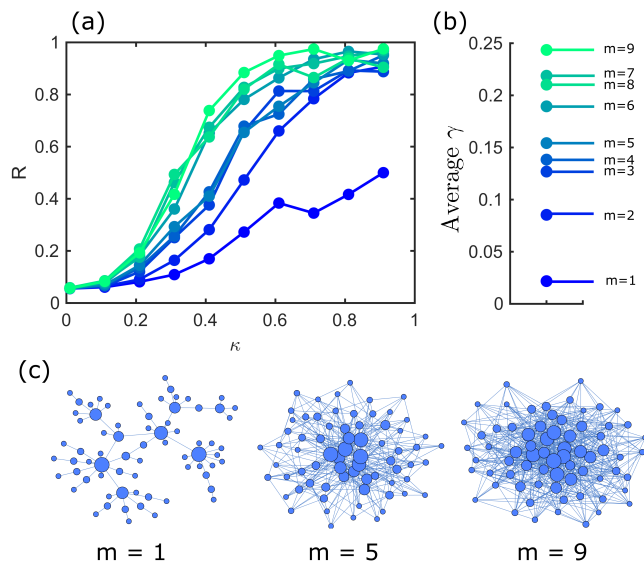
FIG. 4. Frequency synchronization of scale-free networks of identical oscillators and its relation to the spectral gap γ. The scale-free networks are generated from an initial graph with $m+10$ nodes via the preferential attachment mechanism [77]. (a). The onset of frequency synchronization via the dependence of the order parameter R on coupling strength κ. (b). The corresponding average spectral gap, γ, for networks with different m. Each curve in (a) and point in (b) correspond to the average of 100 randomly generated graphs of size $N = 70$ with $m = 1, ..., 9$. Other parameters are as in Fig. 3. A larger spectral gap enhances network synchronizability. (c). Sample scale-free networks with $m = 1, 5, 9$. The size of each node is proportional to its degree.

the chain graph $\gamma = s_2 - s_1 = 1 - \cos{(\pi/N)}$, which for large N can be approximated as π^2/N^2 [76]. For the square lattice graph, the gap is $\gamma = 1 - \cos{(\pi/\sqrt{N})}$ and for large N it is approximated by π^2/N. The star graph's gap is constant and equal to 1. Finally, for the full bipartite graph the gap is $\gamma = N/2$ for even N and $\gamma = N - 2$ for odd N. Figure 3 indicates that the spectral network criterion (7) predicts the scaling of the coupling threshold rather precisely.

To further illustrate the critical role of the spectral gap γ in frequency synchronization, we generated ensembles of uniformly connected, Barabasi-Albert scale-free networks [77]. Figure 4 shows that more heterogeneous networks with higher node degree hubs, in general, correspond to a larger spectral gap γ, and such networks are easier to synchronize.

IV. EXTENSION TO NONIDENTICAL LASER OSCILLATORS

While the criterion (7) performs remarkably well for a large spectrum of the regular and scale-free networks depicted in Figs. 3-4, it is important to point to the lim-

itations of its predictive power. The energy landscape governing the system of repulsively coupled identical oscillators via a hypothetical Lyapunov function may be a non-convex function. As a result, the fundamental eigenmode might not necessarily be the one to win the lasing competition or have the maximal overlap with the lasing mode. Therefore, any mth eigenmode with the corresponding eigenvalue s_m cannot be completely ruled out as unimportant for the network synchronizability. This might become particularly important for the case of nonidentical laser oscillators where the signless Laplacian matrix Q alone does not determine the results. In fact, in the general case, the spectral gap that is predicted to control frequency synchronization of non-identical laser models can be defined as the separation between the real parts of the two eigenvalues of matrix M with the smallest real parts, i.e.,

$$\gamma_M = \Re[\lambda_2 - \lambda_1]. \tag{8}$$

Note that the spectral gap γ_M depends on the coupling coefficient κ present in the complex matrix M. Therefore, the spectral criterion (7) cannot be directly extended to non-identical oscillators. Instead, the spectral gap criterion (8) for non-identical oscillators may serve as a metric that characterizes the synchronizability of the network at a given coupling strength k, with higher values of γ_M corresponding to better synchronizability. For the two-oscillator network in Fig. 2 with frequency detunings $\omega_1 = \omega_0 - \Delta$ and $\omega_2 = \omega_0 + \Delta$, the spectral gap is $\gamma_M = 2\sqrt{\kappa^2 - \Delta^2}$, yielding the above-mentioned threshold coupling $\kappa_c = \Delta$ (see Section V in [18] for the details of this linear stability analysis). Notably, the synchronization threshold is marked with a phase transition in the eigenvalues of matrix M that dictates the system's linearized dynamics.

To verify the general approximate criterion (8) for larger networks, we have numerically calculated the coupling threshold κ_c for all possible 21 network topologies of size $N = 5$ and $1,000$ combinations of random frequency detunings. Figure 5 shows that the networks $1, 2$, and 3, similar to their identical oscillator counterparts with the zero spectral gap $\gamma = 0$, cannot support frequency synchronization for any of the chosen frequency detunings. Remarkably, these networks include a locally coupled ring and an all-to-all network representing two opposite ends of the network topology range and are known to be frequency or phase-synchronizable in attractive phase oscillator networks [34]. It is also worth noting a striking effect that adding one link to the local chain of Fig. 3 top that completes the loop yields the unsynchronizable ring network 2 of Fig. 5. Out of the remaining 18 networks with non-zero spectral gap γ, and therefore, capable of frequency synchronization according to the spectral criterion, only one, the network 18, does not follow the prediction. It remains unsynchronizable for any κ. This is the case where a complex interplay between the network structure and distributions of frequency detuning prevents each mth eigenmodes with eigenvalue λ_m,
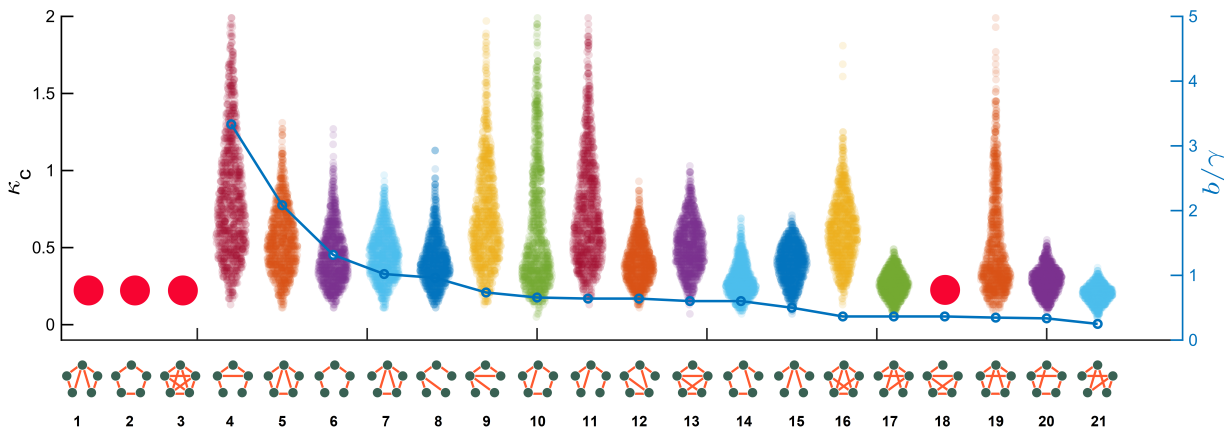
FIG. 5. Synchronization threshold κ_c for all 21 possible connected networks of five detuned oscillators. The scattered points in each violin plot represent the coupling thresholds for $1{,}000$ random frequency distributions with $\omega_m \in \mathcal{U}(-0.5, 0.5)$. The corresponding network is shown under each plot. The large red circles indicate an infinite coupling threshold corresponding to non-synchronizable networks. The networks are ordered from 1 to 21 by the spectral gap γ. The full bipartite network with index 21 has the largest γ. As a reference, the blue line shows a predicted trend from the spectral criterion for identical oscillators (7), with the scaling constant b calculated from the lowest value of κ_c for full bipartite network 21.
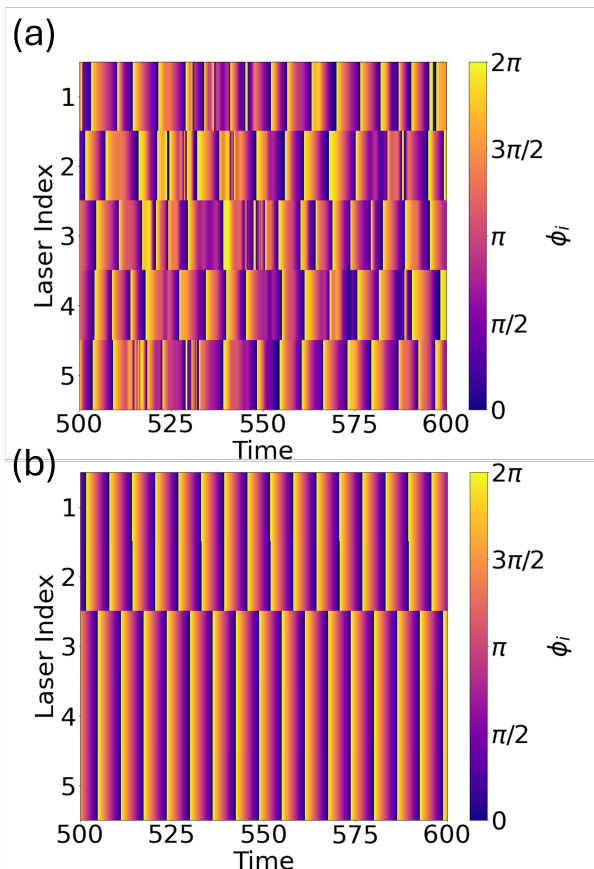

FIG. 6. Phase color plots for the five-oscillator global network (graph 3) and full bipartite network (graph 21) in Fig. 5. (a) Unsynchronizable dynamics in the global network. (b) Frequency synchronization in the form of a two-cluster synchronization state in the full bipartite network. Coupling strength $\kappa = 0.2$.

$m = 1, ..., N$ from becoming the lasing mode. Nonetheless, as in the identical oscillator case, the spectral criterion singles out the full bipartite network (network 21) as the optimal network topology with the lowest synchronization threshold. Its dynamics is contrasted to its globally coupled, unsynchronizable counterpart in Fig. 6.

To better relate the dependence of the threshold κ_c to the identical oscillator criterion (7), we choose the lowest value of κ_c for the full bipartite network (the lowest peak of the corresponding violin plot in Fig. 5) to identify the lowest scaling constant b which could correspond to identical oscillators. We then use this scaling factor via (7) for all other networks to demonstrate how this trend compares to the actual heterogeneous oscillators (Fig. 5). Notably, with a few exceptions, even the identical oscillator spectral criterion can predict the general dependence on the spectral network gap γ. The discrepancy between the predicted trend and the numerical data is due to multiple factors, including different spectral gaps γ_M that depend on the coupling κ and detuning distributions.

V. RELATION TO REPULSIVE KURAMOTO NETWORKS

The spectral gap criterion (8) for frequency synchronization in the amplitude-phase laser model (4) also successfully identifies the full bipartite network as the optimal network topology for frequency synchronization in the Kuramoto-type model obtained from the phase equation in system (4) by setting $A_n = A_m = 1$ (Fig. 7). Note the similarities and differences between the synchronization properties of the full amplitude-phase model (4) (Fig. 5) and its Kuramoto-type counterpart (Fig. 7). Remarkably, the spectral gap criterion can, with a few exceptions, qualitatively characterize the dependence of

the synchronization threshold on the Kuramoto network topology. The most notable exception is the locally coupled network (graph 2 in Figs. 5 and 7) that is unsynchronizable in the amplitude-phase laser network and synchronizable in the phase network. This discrepancy is due to a highly heterogeneous distribution of amplitudes $A_n(t)$ in the amplitude-phase model (4) with local coupling. We use frequency synchronization as a general term that can account for non-stationary but bounded phase dynamics and various phase-locked patterns, including phase clusters, as shown in Fig. 6. As a result, the coupling thresholds for the amplitude-phase model depicted in Fig. 5 correspond to different distributions of non-stationary or stationary amplitudes A_n. Yet, the spectral gap captures the interplay between frequency synchronization of the phase models with uniform distributions and network topologies relatively well.

VI. CONCLUSIONS

In this work, we revealed a general approximate principle that relates a critical coupling threshold for frequency synchronization in repulsive class-A laser networks to the spectral gap between the smallest eigenvalues of the matrix combined from the signless Laplacian connectivity and frequency detuning matrices. The discovered principle demonstrates that the spectral gap of the signless Laplacian, rather than mere connectivity, is a powerful indicator of the synchronizability of such repulsive networks. Applying the spectral principle, we discovered that, in stark contrast with attractive networks, both local ring and global network structures prevent frequency synchronization, whereas the fully bipartite network has optimal synchronization properties. The spectral principle has limitations, as it does not always rule out the synchronizability of a complex network of heterogeneous optical oscillators. However, it identifies topologies that can be easily synchronized and used for scalable designs of large optical oscillator arrays. Moreover, a maximal spectral gap of the complex matrix incorporating frequency detunings could be used as a guiding principle for machine learning approaches to designing disordered laser oscillator networks with optimal synchronization properties required for effective optical computing. While phase synchronization in oscillator networks generally requires frequency synchronization, the reverse is not necessarily true. Achieving frequency synchronization via the optimal network design may create conditions conducive to phase-locking, which is desirable in high-power laser array applications. While injection locking is a well-established technique for laser synchronization [78], it relies on an external master laser and can introduce complexity and scalability issues in large networks. Our study explores self-synchronization mechanisms inherent in the network's topology and coupling, which can offer advantages in terms of robustness and scalability for applications like distributed optical computing. Beyond optical networks, our spectral network principle is applicable to a broader class of physical and biological oscillators, including Kuramoto networks, which have wide-ranging applications in neuroscience, biology, and engineering.

[1] M. Nixon, E. Ronen, A. A. Friesem, and N. Davidson, Observing geometric frustration with thousands of coupled lasers, Phys. Rev. Lett. **110**, 184102 (2013).

[2] V. Eckhouse, M. Fridman, N. Davidson, and A. A. Friesem, Loss enhanced phase locking in coupled oscillators, Phys. Rev. Lett. **100**, 024102 (2008).

[3] M. Honari-Latifpour and M.-A. Miri, Mapping the xy hamiltonian onto a network of coupled lasers, Phys. Rev. Research **2**, 043335 (2020).

[4] M. Parto, W. Hayenga, A. Marandi, D. N. Christodoulides, and M. Khajavikhan, Realizing spin hamiltonians in nanoscale active photonic lattices, Nature Materials **19**, 725 (2020).

[5] J. R. Fienup, Phase retrieval algorithms: a comparison, Appl. Opt. **21**, 2758 (1982).

[6] J. Leger, Diode Laser Arrays, edited by D. Botez and D. Scifres (1994).

[7] J. Thévenin, M. Romanelli, M. Vallet, M. Brunel, and T. Erneux, Resonance assisted synchronization of coupled oscillators: frequency locking without phase locking, Physical Review Letters **107**, 104101 (2011).

[8] R. Roy and K. S. Thornburg Jr, Experimental synchronization of chaotic lasers, Physical Review Letters **72**, 2009 (1994).

[9] N. Nair, K. Hu, M. Berrill, K. Wiesenfeld, and Y. Braiman, Using disorder to overcome disorder: A mechanism for frequency and phase synchronization of diode laser arrays, Phys. Rev. Lett. **127**, 173901 (2021).

[10] Y. Shen, N. C. Harris, S. Skirlo, M. Prabhu, T. Baehr-Jones, M. Hochberg, X. Sun, S. Zhao, H. Larochelle, D. Englund, et al., Deep learning with coherent nanophotonic circuits, Nature photonics **11**, 441 (2017).

[11] M. Aspelmeyer, T. J. Kippenberg, and F. Marquardt, Cavity optomechanics, Reviews of Modern Physics **86**, 1391 (2014).

[12] A. Pasquazi, M. Peccianti, L. Razzari, D. J. Moss, S. Coen, M. Erkintalo, Y. K. Chembo, T. Hansson, S. Wabnitz, P. Del'Haye, et al., Micro-combs: A novel generation of optical sources, Physics Reports **729**, 1 (2018).
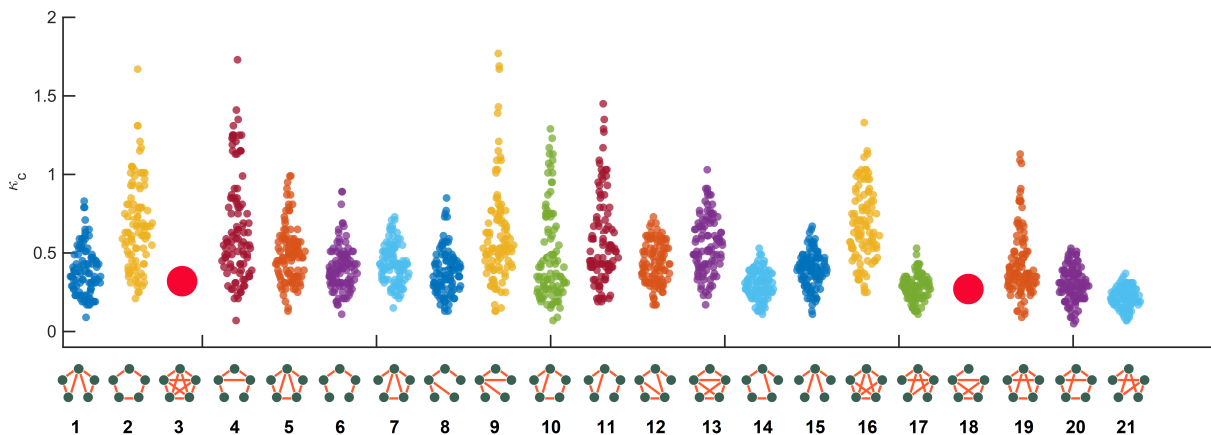
FIG. 7. Synchronization threshold κ_c for all 21 possible connected networks of five detuned Kuramoto-type phase model oscillators obtained from the phase equation (3) by setting $A_n = A_m = 1$. The notations and simulation parameters are as in Fig. 5. Note that the phase model networks generally have similar synchronization properties determined by the spectral gap as their full model counterparts of Fig. 5, except for the locally coupled ring (graph 3) and graphs 1 and 18.

[13] S. A. Diddams, K. Vahala, and T. Udem, Optical frequency combs: Coherently uniting the electromagnetic spectrum, Science **369**, eaay3676 (2020).

[14] N. G. Berloff, M. Silva, K. Kalinin, A. Askitopoulos, J. D. Töpfer, P. Cilibrizzi, W. Langbein, and P. G. Lagoudakis, Realizing the classical XY Hamiltonian in polariton simulators, Nature Materials **16**, 1120 (2017).

[15] M. Nixon, M. Fridman, E. Ronen, A. A. Friesem, N. Davidson, and I. Kanter, Controlling synchronization in large laser networks, Phys. Rev. Lett. **108**, 214101 (2012).

[16] M. Nixon, M. Friedman, E. Ronen, A. A. Friesem, N. Davidson, and I. Kanter, Synchronized cluster formation in coupled laser networks, Phys. Rev. Lett. **106**, 223901 (2011).

[17] D. Brunner and I. Fischer, Reconfigurable semiconductor laser networks based on diffractive coupling, Opt. Lett. **40**, 3854 (2015).

[18] J. Ding, I. Belykh, A. Marandi, and M.-A. Miri, Dispersive versus dissipative coupling for frequency synchronization in lasers, Phys. Rev. Applied **12**, 054039 (2019).

[19] T. Wang and J. Roychowdhury, Oim: Oscillator-based ising machines for solving combinatorial optimisation problems, in *Unconventional Computation and Natural Computation*, edited by I. McQuillan and S. Seki (Springer International Publishing, Cham, 2019) pp. 232–256.

[20] Z. Wang, A. Marandi, K. Wen, R. L. Byer, and Y. Yamamoto, Coherent Ising machine based on degenerate optical parametric oscillators, Phys. Rev. A **88**, 063853 (2013).

[21] A. Lucas, Ising formulations of many NP problems, Frontiers in Physics **2**, 5 (2014).

[22] M.-A. Miri and V. Menon, Neural computing with coherent laser networks, Nanophotonics **12**, 883 (2023).

[23] A. Andrianov, N. Kalinin, E. Anashkina, and G. Leuchs, Highly efficient coherent beam combining of tiled aperture arrays using out-of-phase pattern, Opt. Lett. **45**, 4774 (2020).

[24] Y. Braiman, J. F. Lindner, and W. L. Ditto, Taming spatiotemporal chaos with disorder, Nature **378**, 465 (1995).

[25] L. Fabiny, P. Colet, R. Roy, and D. Lenstra, Coherence and phase dynamics of spatially coupled solid-state lasers, Phys. Rev. A **47**, 4287 (1993).

[26] K. S. Thornburg, M. Möller, R. Roy, T. W. Carr, R.-D. Li, and T. Erneux, Chaos and coherence in coupled lasers, Phys. Rev. E **55**, 3865 (1997).

[27] G. Kozyreff, A. Vladimirov, and P. Mandel, Global coupling with time delay in an array of semiconductor lasers, Phys. Rev. Lett. **85**, 3809 (2000).

[28] J. Zamora-Munt, C. Masoller, J. Garcia-Ojalvo, and R. Roy, Crowd synchrony and quorum sensing in delay-coupled lasers, Phys. Rev. Lett. **105**, 264101 (2010).

[29] S. Mahler, A. A. Friesem, and N. Davidson, Experimental demonstration of crowd synchrony and first-order transition with lasers, Phys. Rev. Research **2**, 043220 (2020).

[30] L. M. Pecora and T. L. Carroll, Master stability functions for synchronized coupled systems, Phys. Rev. Lett. **80**, 2109 (1998).

[31] S. Boccaletti, J. Kurths, G. Osipov, D. Valladares, and C. Zhou, The synchronization of chaotic systems, Physics Reports **366**, 1 (2002).

[32] V. N. Belykh, I. V. Belykh, and M. Hasler, Connection graph stability method for synchronized coupled chaotic systems, Physica D: Nonlinear Phenomena **195**, 159 (2004).

[33] J. Sun, E. M. Bollt, and T. Nishikawa, Master stability functions for coupled nearly identical dynamical systems, Europhysics Letters **85**, 60011 (2009).

[34] J. G. Restrepo, E. Ott, and B. R. Hunt, Onset of synchronization in large networks of coupled oscillators, Phys. Rev. E **71**, 036151 (2005).

[35] T. Nishikawa and A. E. Motter, Network synchronization landscape reveals compensatory structures, quantization, and the positive effect of negative interactions, Proceedings of the National Academy of Sciences **107**, 10342 (2010).

[36] S. Boccaletti, V. Latora, Y. Moreno, M. Chavez, and D.-U. Hwang, Complex networks: Structure and dynamics,

Physics Reports **424**, 175 (2006).

[37] F. Sorrentino and M. Porfiri, Analysis of parameter mismatches in the master stability function for network synchronization, Europhysics Letters **93**, 50002 (2011).

[38] G. B. Ermentrout, Stable periodic solutions to discrete and continuum arrays of weakly coupled nonlinear oscillators, SIAM Journal on Applied Mathematics **52**, 1665 (1992).

[39] F. C. Hoppensteadt and E. M. Izhikevich, *Weakly connected neural networks*, Vol. 126 (Springer Science & Business Media, 2012).

[40] E. M. Izhikevich, *Dynamical systems in neuroscience* (MIT press, 2007).

[41] I. Belykh, E. de Lange, and M. Hasler, Synchronization of bursting neurons: What matters in the network topology, Phys. Rev. Lett. **94**, 188101 (2005).

[42] I. Belykh, R. Reimbayev, and K. Zhao, Synergistic effect of repulsive inhibition in synchronization of excitatory networks, Phys. Rev. E **91**, 062919 (2015).

[43] P. C. Matthews and S. H. Strogatz, Phase diagram for the collective behavior of limit-cycle oscillators, Physical Review Letters **65**, 1701 (1990).

[44] P. C. Matthews, R. E. Mirollo, and S. H. Strogatz, Dynamics of a large system of coupled nonlinear oscillators, Physica D: Nonlinear Phenomena **52**, 293 (1991).

[45] W. Shing Lee, E. Ott, and T. M. Antonsen, Phase and amplitude dynamics in large systems of coupled oscillators: Growth heterogeneity, nonlinear frequency shifts, and cluster states, Chaos: An Interdisciplinary Journal of Nonlinear Science **23** (2013).

[46] H. Nakao and A. S. Mikhailov, Diffusion-induced instability and chaos in random oscillator networks, Physical Review E—Statistical, Nonlinear, and Soft Matter Physics **79**, 036214 (2009).

[47] J. A. Acebrón, L. L. Bonilla, C. J. P. Vicente, F. Ritort, and R. Spigler, The Kuramoto model: A simple paradigm for synchronization phenomena, Reviews of Modern Physics **77**, 137 (2005).

[48] R. E. Mirollo and S. H. Strogatz, The spectrum of the locked state for the Kuramoto model of coupled oscillators, Physica D: Nonlinear Phenomena **205**, 249 (2005).

[49] A. Arenas, A. Diaz-Guilera, and C. J. Pérez-Vicente, Synchronization reveals topological scales in complex networks, Phys. Rev. Lett. **96**, 114102 (2006).

[50] F. Dörfler and F. Bullo, Synchronization in complex networks of phase oscillators: A survey, Automatica **50**, 1539 (2014).

[51] G. S. Medvedev and X. Tang, Stability of twisted states in the kuramoto model on cayley and random graphs, Journal of Nonlinear Science **25**, 1169 (2015).

[52] F. A. Rodrigues, T. K. D. Peron, P. Ji, and J. Kurths, The Kuramoto model in complex networks, Physics Reports **610**, 1 (2016).

[53] T. Nishikawa and A. E. Motter, Symmetric states requiring system asymmetry, Phys. Rev. Lett. **117**, 114101 (2016).

[54] Y. Zhang, J. L. Ocampo-Espindola, I. Z. Kiss, and A. E. Motter, Random heterogeneity outperforms design in network synchronization, Proceedings of the National Academy of Sciences **118**, e2024299118 (2021).

[55] P. S. Skardal, D. Taylor, and J. Sun, Optimal synchronization of complex networks, Phys. Rev. Lett. **113**, 144101 (2014).

[56] Y. Zhang and A. E. Motter, Identical synchronization of nonidentical oscillators: When only birds of different feathers flock together, Nonlinearity **31**, R1 (2017).

[57] A. Nazerian, S. Panahi, and F. Sorrentino, Synchronization in networks of coupled oscillators with mismatches, Europhysics Letters **143**, 11001 (2023).

[58] R. Berner, S. Yanchuk, Y. Maistrenko, and E. Schöll, Generalized splay states in phase oscillator networks, Chaos: An Interdisciplinary Journal of Nonlinear Science **31**, 073128 (2021).

[59] R. Ronge and M. A. Zaks, Splay states and two-cluster states in ensembles of excitable units, The European Physical Journal Special Topics **230**, 2717 (2021).

[60] V. O. Munyayev, M. I. Bolotov, L. A. Smirnov, G. V. Osipov, and I. Belykh, Cyclops states in repulsive kuramoto networks: the role of higher-order coupling, Phys. Rev. Lett. **130**, 107201 (2023).

[61] L. Tsimring, N. Rulkov, M. Larsen, and M. Gabbay, Repulsive synchronization in an array of phase oscillators, Phys. Rev. Lett. **95**, 014101 (2005).

[62] A. Pikovsky, M. Rosenblum, and J. Kurths, *Synchronization: a Universal Concept in Nonlinear Sciences*, Vol. 12 (Cambridge University Press, 2003).

[63] F. Arecchi, G. Lippi, G. Puccioni, and J. Tredice, Deterministic chaos in laser with injected signal, Optics Communications **51**, 308 (1984).

[64] F. T. Arecchi, G. Giacomelli, A. Lapucci, and R. Meucci, Dynamics of a CO_2 laser with delayed feedback: The short-delay regime, Phys. Rev. A **43**, 4997 (1991).

[65] M. Born, E. Wolf, A. B. Bhatia, P. C. Clemmow, D. Gabor, A. R. Stokes, A. M. Taylor, P. A. Wayman, and W. L. Wilcock, *Principles of Optics: Electromagnetic Theory of Propagation, Interference and Diffraction of Light*, 7th ed. (Cambridge University Press, 1999).

[66] W. E. Lamb Jr, Theory of an optical maser, Physical Review **134**, A1429 (1964).

[67] G. P. Agrawal and N. K. Dutta, *Long-wavelength semiconductor lasers*, Vol. 1 (Springer, 1986).

[68] J. R. Tredicce, F. T. Arecchi, G. L. Lippi, and G. P. Puccioni, Instabilities in lasers with an injected signal, JOSA B **2**, 173 (1985).

[69] M.-A. Miri and V. Menon, Neural computing with coherent laser networks, Nanophotonics **12**, 883 (2023).

[70] A. M. Yacomotti, Z. Denis, A. Biella, and C. Ciuti, Quantum density matrix theory for a laser without adiabatic elimination of the population inversion: Transition to lasing in the class-B limit, Laser & Photonics Reviews **17**, 2200377 (2023).

[71] I. Amelio and I. Carusotto, Theory of the coherence of topological lasers, Physical Review X **10**, 041060 (2020).

[72] E. R. van Dam and W. H. Haemers, Which graphs are determined by their spectrum?, Linear Algebra and its Applications **373**, 241 (2003).

[73] D. Cvetković, P. Rowlinson, and S. K. Simić, Signless Laplacians of finite graphs, Linear Algebra and its Applications **423**, 155 (2007).

[74] D. Cvetković and S. K. Simić, Towards a spectral theory of graphs based on the signless Laplacian, ii, Linear Algebra and its Applications **432**, 2257 (2010).

[75] M. Desai and V. Rao, A characterization of the smallest eigenvalue of a graph, Journal of Graph Theory **18**, 181 (1994).

[76] J. Ding and M.-A. Miri, Mode discrimination in dissipatively coupled laser arrays, Opt. Lett. **44**, 5021 (2019).

[77] R. Albert and A.-L. Barabási, Statistical mechanics of complex networks, Rev. Mod. Phys. **74**, 47 (2002).

[78] R. Lang, Injection locking properties of a semiconductor laser, IEEE Journal of Quantum Electronics **18**, 976 (1982).